

The Nucleation and Suppression of Transformation Twinning in Barium Sodium Niobate

A. W. VERE, J. G. PLANT, B. COCKAYNE
Royal Radar Establishment, Malvern, Worcs, UK

K. G. BARRACLOUGH, I. R. HARRIS
Department of Physical Metallurgy and Science of Materials, University of Birmingham, UK

Received 16 June 1969

It has already been established that the microtwinning associated with the tetragonal to orthorhombic phase transition in barium sodium niobate can be suppressed by cooling from above the transformation temperature under an applied stress. The work reported here indicates that the quotation of specific stress values for this process is misleading since, for any specimen, there is an optimum range of applied stress over which complete suppression of the microtwinning is achieved. This range is shown to be dependent upon the particular twin density and distribution which is determined by the presence of other crystal defects and by the composition of the material. Means of reducing the twin density are also discussed.

An anomalous expansion behaviour in the [001] crystal direction, detected by a dilatometric technique, is consistent with the observed tendency to crack as the material is cooled through the Curie point.

1. Introduction

Current interest in mixed-oxide crystals for use in non-linear optical devices [1, 2] has led to considerable research effort on the growth of barium sodium niobate (nominal* formula $\text{Ba}_2\text{NaNb}_5\text{O}_{15}$) [3, 4]. Recently, modifications to the after-heating arrangement used in the Czochralski crystal-growth technique have made possible the production of crack-free single crystals of good optical quality $\text{Ba}_2\text{NaNb}_5\text{O}_{15}$ up to 4 cm in length and approximately 1.5 cm in diameter [5].

One defect which impairs the device performance of this material is the occurrence of microtwinning associated with the tetragonal (4 mm) to orthorhombic (mm 2) phase transformation at approximately 260° C [6].

Twinning occurs on $(100)_T$ † and $(010)_T$ planes, dividing the original crystal into a series of rectangular-based prisms, the major direction of which lies parallel to the $[001]_T$ axis. Examination of these crystallites shows that the $[100]$ direction of the orthorhombic unit cell lies at 45° to the $[100]$ direction of the tetragonal cell. Moreover, the crystallites are oriented so that the $[100]_O$ direction on one crystallite is perpendicular to the $[100]_O$ direction in adjacent crystallites (fig. 1).

It has been reported that microtwinning may be suppressed by cooling the crystal from above the transformation temperature under an applied stress of 70 kg cm⁻² [3]. However, the present work shows that the applied stress necessary to achieve complete detwinning varies widely

*Except where otherwise stated the compositions quoted in this paper refer only to the original charge because barium and sodium segregation and sodium loss during crystal growth cause substantial variations in crystal composition. (table I).

†Planes and directions in the tetragonal and orthorhombic unit cells are distinguished by the subscripts T and O respectively.

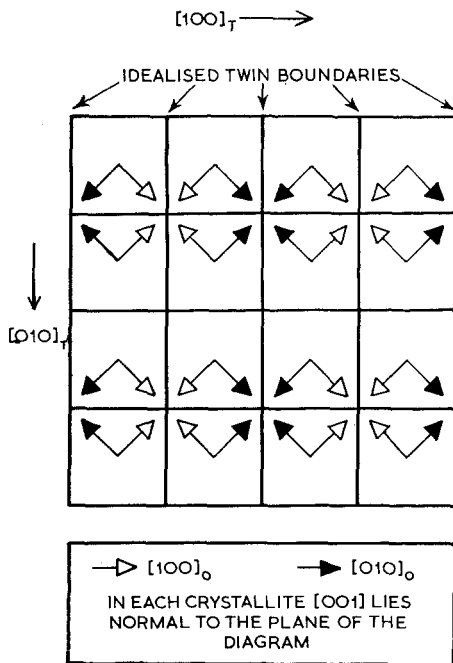


Figure 1 Schematic illustration of the orientation of the orthorhombic unit cell in the crystallites produced by microtwinning.

according to the density and distribution of the twins. Factors affecting these parameters have therefore been studied in some detail.

Dilatometric measurements of the expansion of the material as a function of temperature have also been made in order to gain further information on the nature of the transformation. These results indicate possible reasons for the tendency of the material to crack during cooling through the ferroelectric Curie temperature.

2. Experimental Techniques

Single crystals of barium sodium niobate were produced using a modified Czochralski technique [5]. The crystals were grown in a 100% O_2 environment at a pull rate of 0.5 cm h^{-1} and a rotation rate of 60 rpm.

The mechanical properties of the material were studied on rectangular prism specimens $8 \times 3 \times 3 \text{ mm}$ which were cut with the long dimension parallel to $[110]_T$. The side faces were $(001)_T$ and $(\bar{1}10)_T$. These specimens were located between compression plates in a small Pt-40% Rh resistance-wound furnace mounted on an Instron Universal Testing Machine. A vertical slot was cut in the furnace wall to permit

observation of the specimen while under compression above room temperature. The compression plates were fabricated in "sindanyo", an asbestos-type fibre compound which serves a dual purpose since it deforms sufficiently to ensure overall contact between the specimen and the plate, whilst its good thermal insulation restricts heat loss from the ends of the specimen.

The method used to suppress the formation of microtwins was similar to that outlined by van Uitert *et al* [3]. Specimens were compressed along the $[110]_T$ axis at selected temperatures in the range 240 to 560°C using a heating rate of approximately $500^\circ \text{C h}^{-1}$. After annealing at the test temperature for 20 min each specimen was loaded at a strain rate of 0.05 min^{-1} to a predetermined stress level and subsequently cooled to room temperature under the applied stress.

Information on the structural changes occurring in the temperature range 25 to 800°C was derived from a series of dilatometric measurements of lattice expansion as a function of temperature for the $[001]_T$, $[110]_T$ and $[\bar{1}10]_T$ crystal directions.

To perform the measurements, a rectangular prism specimen approximately $5 \times 4 \times 4 \text{ mm}$ was located against the sealed end of a silica tube and heated in a resistance-wound furnace at a rate of $2^\circ \text{C min}^{-1}$. Changes in the length of the specimen were transmitted to a transducer via a horizontal Vitreosil push-rod and the output from the transducer was fed to a strip-chart recorder. Using this technique, length changes as small as $2 \times 10^{-6} \text{ cm}$ can be detected. The results given are corrected for dimensional changes in the apparatus. These were evaluated in a control experiment using a silica specimen as a standard.

3. Results and Discussion

3.1. The Twinned Orthorhombic Structure

When (001) slices of $\text{Ba}_2\text{NaNb}_5\text{O}_{15}$ are cooled from approximately 500°C to room temperature a gradual crystallographic change occurs. This change is readily studied under linearly polarised light in a hot-stage optical microscope. At about 450°C a diffuse pattern appears in the crystal slice (fig. 2) and becomes increasingly distinct as cooling continues. When viewed in unpolarised light these changes are not detected and are thus attributable to increasing strain within the crystal lattice. At 240°C (260°C during the heating part of the cycle) microtwinning occurs. The twin bands first nucleate at

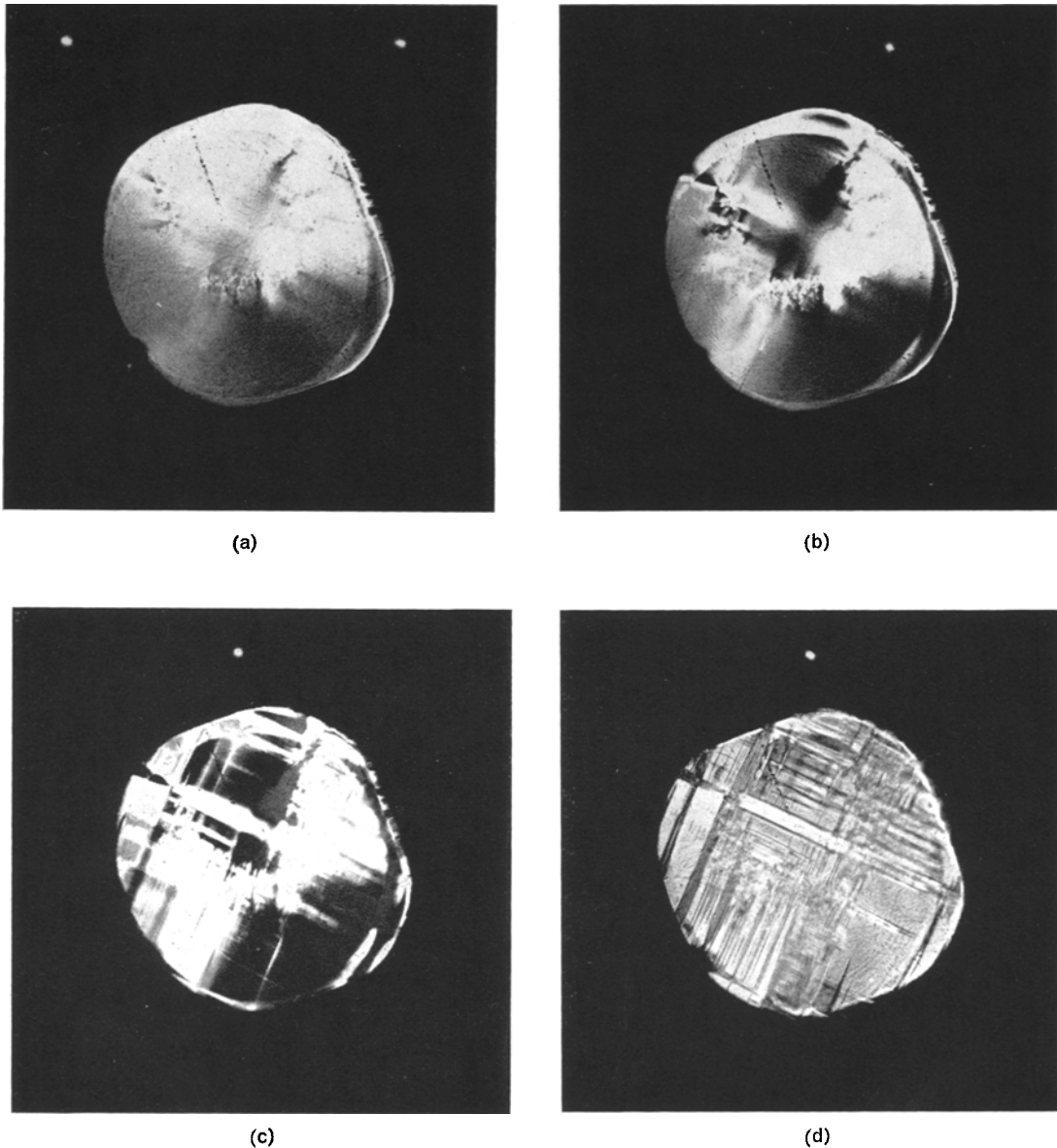


Figure 2 Stages in the transformation from the tetragonal to orthorhombic phase as observed under linearly polarised light. (a) 310°C ; (b) 280°C ; (c) 220°C ; (d) 200°C . Magnification $\times 3$.

defects within the crystal or, in the absence of such defects, in the cooler regions of the crystal slice. The twins propagate rapidly across the specimen in $[010]_T$ and $[100]_T$ directions along (100) and (010) planes, producing a rectangular network (fig. 2d). This crystallographic change is observable in both polarised and unpolarised light. The total extinction condition apparent in regions between the twin bands when viewed between crossed polars indicates that these

regions are strain-free below the "transformation temperature" (fig. 3).

Despite the abruptness of the twin-band nucleation when viewed in unpolarised light the strain patterns observed above the apparent transformation temperature indicate that the transition actually occurs over a wide temperature range. Examination of conoscopic interference patterns produced at high temperatures also indicates that the material transforms gradually

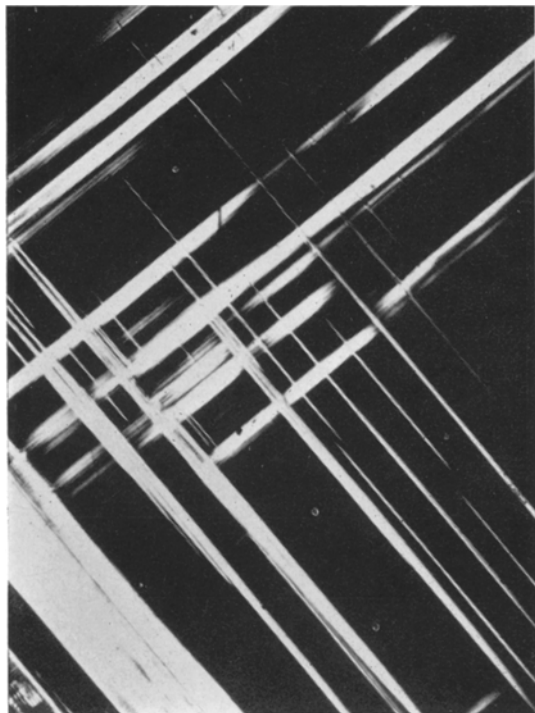


Figure 3 Typical twin-band pattern on (001) slice of $\text{Ba}_2\text{NaNb}_5\text{O}_{15}$ as viewed under crossed polars ($\times 55$).

and continuously over the temperature range 200 to 300° C from the uniaxial structure stable at high temperatures to a biaxial structure stable at room temperature.

A typical expansion curve (fig. 4) shows a slight discontinuity which can be directly related to the formation of microtwins. The temperature at which the discontinuity occurs is slightly dependent on composition and varies over the range 250 to 280° C. During cooling, the observed transition temperatures are approximately 20° C below those obtained on heating, showing good agreement with the observed temperature hysteresis in the disappearance and reappearance of the microtwins as revealed by optical microscopy.

The change in slope of the expansion curve in the 250 to 300° C range is small in comparison to that at the Curie point. This fact and the diffuse nature of the change are indicative of a second order transition, as tentatively suggested by Scott *et al* [7] on the basis of their DTA results.

All the above observations are consistent with the hypothesis that the formation of microtwins during the tetragonal to orthorhombic phase

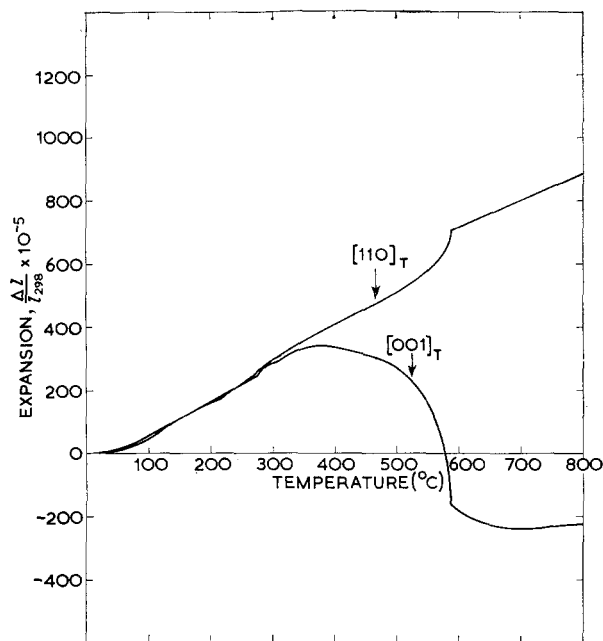


Figure 4 A typical expansion curve for a barium sodium niobate crystal.

transition operates as a strain relieving mechanism. In the transition, the c -axis dimension of the unit cell remains almost constant. The a - and b -axes of the orthorhombic unit cell are of different length, however and a simple transformation without change in orientation would involve a high internal strain. These effects can be minimised by dividing the crystal into a series of prismatic crystallites whose major axes run parallel to the $[001]_T$ directions and in which the direction of the $[100]_O$ axis in one crystallite lies parallel to the direction of the $[010]_O$ axis in the adjacent crystallite (fig. 1).

3.2. The Nucleation of Microtwins

If microtwins are stress-nucleated the twin distribution should be homogeneous in defect-free material. In practice, $(001)_T$ slices show regions in which the twin density is abnormally high. Moreover, on cycling the crystal through the temperature range 25 to 700° C after prolonged annealing at 700° C the twin structure remains unchanged, exhibiting a distinct memory effect. In order to modify the twin-band configuration it is usually necessary to create a new stress-state within the crystal. This can be achieved by changing the crystal dimensions. Even so, the regions of abnormally high twin

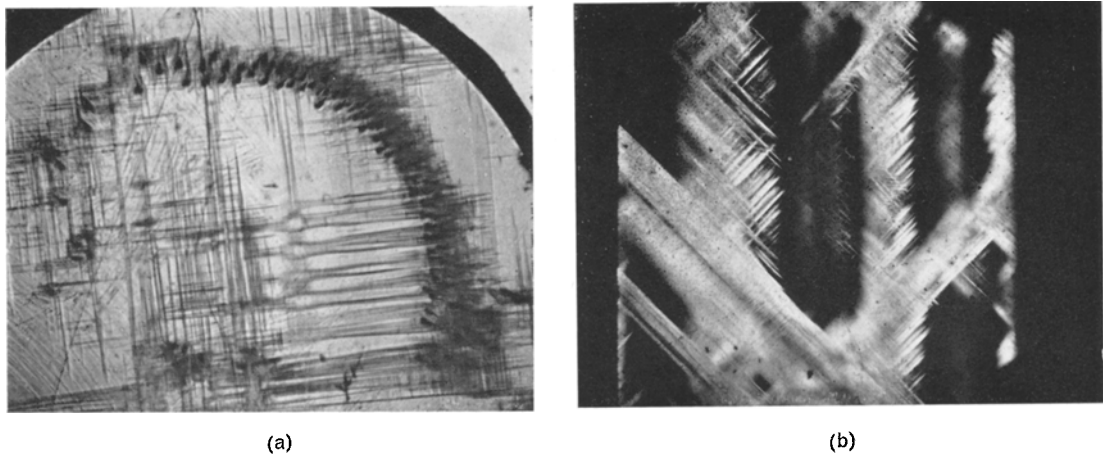


Figure 5 Nucleation of high twin-density regions in areas containing (a) cellular structure ($\times 10$); (b) coarse growth striae ($\times 10$).

density remain relatively unaffected. On cooling through the transformation temperatures these regions act as the initial nucleation sites for twin-band formation. Conversely, the twinned structure is retained longest in these regions during the orthorhombic to tetragonal transition.

Detailed examination of the severely twinned region invariably reveals the presence of some fundamental defect generated at the growth interface during solidification. Thus, cellular structures (fig. 5a) and coarse growth striae (fig. 5b) both act as twin nucleating sites. Regions of high twin density have also been found delineating the edges of interface facets observed in the material.

In some cases, regions of high twin density are caused by the presence of clusters of small defects. On (001) cleavage faces these appear as small overlapping platelets with truncated square or tetragonal cross-sections (fig. 6a). The major sides have a mean length of approximately $150 \mu\text{m}$ and are parallel to $[110]_T$ while the truncations lie along $[100]_T$. When (001)_T faces are etched in a hot concentrated solution of KHF_2 in HNO_3 these defects are delineated by rows of square section etch-pits with sides parallel to $[110]_T$ (fig. 6b). Two types of etch-pit are observed. The first type is shallow and flat-bottomed and usually forms the outline of the defect. The second type is a series of angular pits

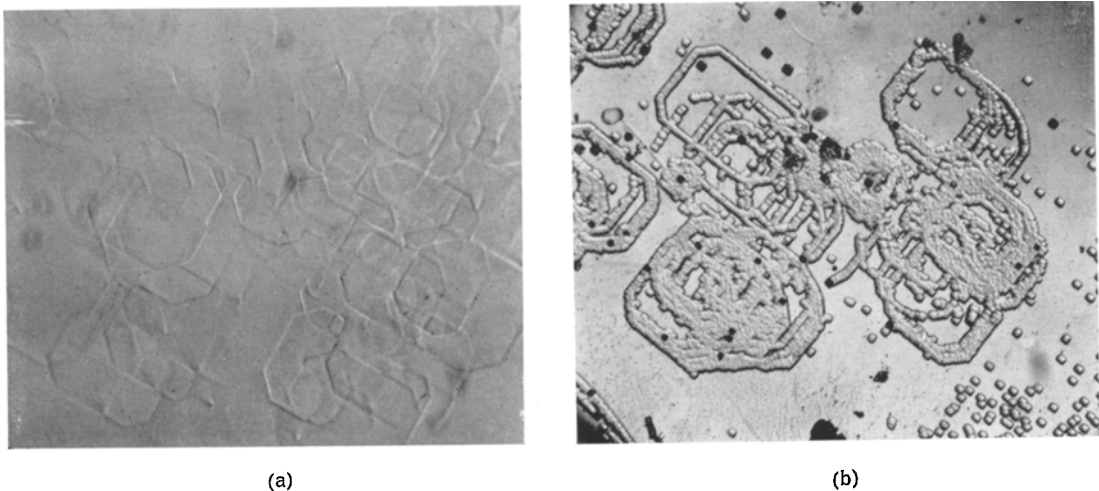


Figure 6 Magnified view of the core defect in $\text{Ba}_2\text{NaNb}_5\text{O}_{15}$; (a) (001) cleavage face ($\times 88$); (b) after etching in KHF_2 dissolved in concentrated HNO_3 ($\times 114$).

which appear in darker contrast; these frequently occur at the end of a series of flat-bottomed pits or at the intersection of twin boundaries. In addition to the square or rectangular defects described above, etch-pit spirals (fig. 7) are occasionally observed. These are similar in size and orientation to the simpler forms.

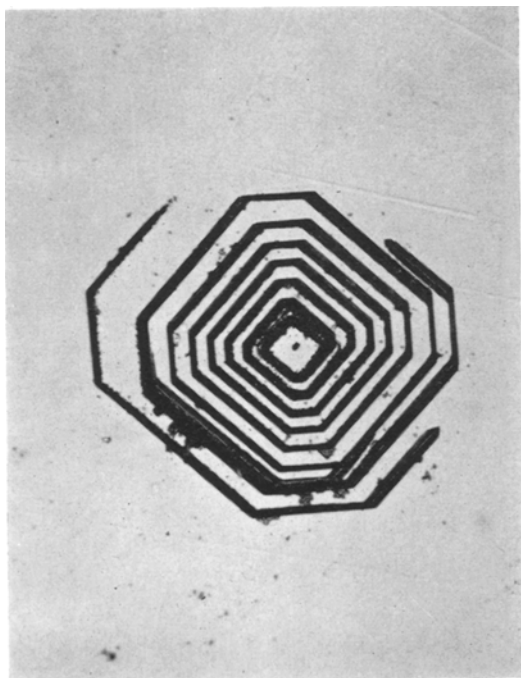


Figure 7 Etch-pit spiral on (001) face ($\times 270$).

The defects are frequently found in clusters in the central region of the crystal. Examination of several (001) sections cut from the same crystal establishes that the defect is a line defect which, in the case of the central cluster, nucleates at the original seed crystal and penetrates several centimetres into the growing crystal. Furthermore, the outline of the defective region corresponds in both length and orientation to the position of those faces of the seed crystal produced by abrasive cutting on a diamond-saw. Fig. 8 shows the pattern obtained on an (001) face of a slice cut from a [001] growth-axis crystal approximately one centimetre below the original seed, the outline of which is clearly defined. The close association between the location of the etch-pit defects and the cut edges of the seed crystal implies that the defects are

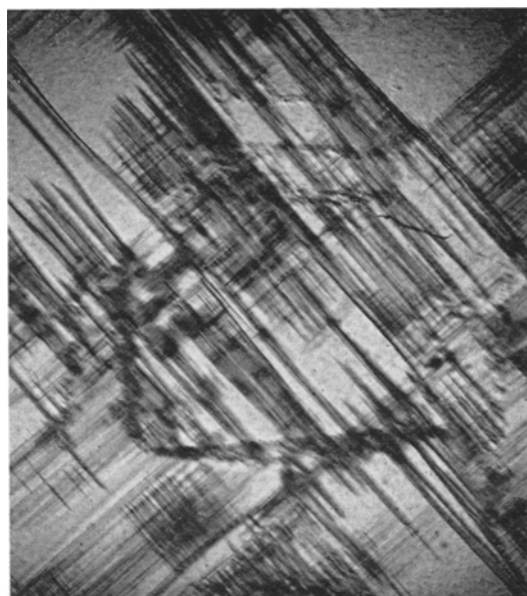


Figure 8 Increased twin-density around defective region delineating the original seed crystal ($\times 14$).

produced by the propagation of surface damage on the seed into the growing crystal. Such propagation may take the form of dislocations of large Burgers vector. The points at which the dislocations emerge on the growth interface would undoubtedly produce an atomic-scale perturbation on the interface, thereby providing a possible nucleation site for localised spiral growth of the type proposed by Frank [8]. Growth of this type is most likely to occur on faceted regions where nucleation is restricted.

3.3. The Mechanical Properties of $\text{Ba}_2\text{NaNb}_5\text{O}_{15}$

In order to eliminate the microtwinning arising from the tetragonal to orthorhombic transformation it is necessary to cool the material from above the transformation temperature under an applied stress. Several preliminary experiments were performed to investigate the mechanical properties of the material.

The upper temperature limit for effective detwinning of $\text{Ba}_2\text{NaNb}_5\text{O}_{15}$ is the ferroelectric Curie point at about 580°C . Specimens cooled from above this temperature contain several ferroelectric domains of opposite polarity which are detrimental to device performance. Moreover, the material shows an increased tendency to crack in the temperature region around the

Curie point. A possible explanation of this enhanced susceptibility to cracking is suggested by the variation in the expansion rate of the material as a function of temperature (fig. 4). The crystal expands continuously over the temperature range 25 to 380°C. At the latter temperature, the [001] axis begins to contract and the rate of contraction increases rapidly up to a temperature of 585°C. At this temperature there is an abrupt decrease in the rate of contraction of the [001] axis and a similar discontinuity in the expansion of the $[110]_T$ and $[\bar{1}10]_T$ axes. (The expansion curves for $[110]$ and $[\bar{1}10]$ crystal directions are virtually coincident. For clarity, only the $[110]$ curve is shown in fig. 4). The temperature at which this occurs is in close agreement with the Curie temperature determined from hot-stage microscopy and differential thermal analysis.

Since the material shows tetragonal symmetry above approximately 300°C, the shape of the $[001]_T$ expansion curve is directly related to the change in axial ratio, c/a , and volume, a^2c , of the tetragonal unit cell. Hence there is a substantial contraction of the unit cell during heating through the Curie temperature and it is probable that the internal strain generated during this rapid volume change causes fracture.

The predominant fracture plane in the material is $(001)_T$ although $[110]_T$ cracking is also frequently observed. Although, as indicated above, the crystal suffers maximum internal strain during cooling through the temperature range 550 to 600°C, the thermal shock resistance is low throughout the temperature range from room temperature to the melting point. This is particularly so in crystals containing defects, which act as fracture nucleation sites. Specimens compressed along the $[110]_T$ axis at strain rates above 0.002 min^{-1} in the temperature range 25 to 600°C show no evidence of plastic deformation prior to brittle fracture on $(110)_T$ and $(001)_T$. The room temperature fracture stress exceeds 1000 kg cm^{-2} .

3.4. Removal of Twinning by Uniaxial Compression

Van Uitert *et al* [3] have recently reported that the microtwinning can be suppressed by the application of an external stress equal to 70 kg cm^{-2} at 250°C with subsequent cooling to room temperature under the applied stress. In practice the situation is considerably more complex because the applied stress is directly related to the density and distribution of the

microtwins. For each specimen there is a range of applied stress, within which complete detwinning of the specimen can be achieved, provided that a uniform stress state has been established within the specimen. Below this range the applied stress has little or no effect on the twin structure generated during the transformation. If the applied stress lies above the upper limit of the optimum stress range, the twin density obtained during cooling through the transformation temperature is increased. Finally, stresses exceeding the room temperature compressive fracture stress for the specimen give rise to rapid twin generation during cooling, culminating in brittle fracture by twin-plane parting.

The optimum stress-range for detwinning occurs at an increasing stress level as the twin density increases. Fig. 9 shows the values obtained for some twenty crystals. Specimens which have

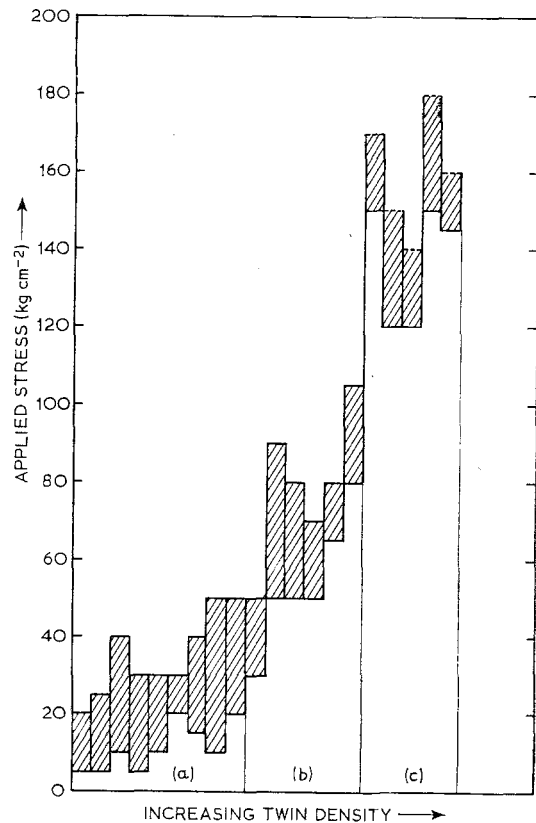


Figure 9 Graph showing the optimum applied-stress range for detwinning as a function of twin density. (a) Uniform, low twin density. (b) Isolated regions of abnormally high twin density. (c) Abnormally high twin density throughout the volume of the crystal.

optimum stress ranges at low applied-stress levels (fig. 9 (a)) all exhibit a low twin density and a uniform twin-band distribution, whereas those for which complete detwinning can only be achieved by application of a high external stress (fig. 9(c)) show an abnormally high twin density throughout the specimen, resulting from the presence of a high concentration of crystal defects of the types described in section 3.2. Specimens in the intermediate range (b) contain isolated regions of abnormally high twin-density. Hence, although it is possible to obtain either partial or complete detwinning of high twin density specimens, the exercise is rather academic in character since the applied stress has no effect upon the crystal defects which are the fundamental cause of twin nucleation.

Studies have also been made of the effect of various test temperatures and cooling rates on the efficiency of the detwinning process. The microtwinning appears to be independent of cooling rate within the range $0.5^{\circ}\text{C min}^{-1}$ to $20^{\circ}\text{C min}^{-1}$. Similarly, no marked differences have been recorded for test temperatures ranging from 260 to 560°C . No improvement in crystal perfection was achieved using temperatures below 260°C and it is concluded that the test temperature must exceed the transformation temperature to obtain successful detwinning. The observed independence of test temperature and cooling rate in the relevant ranges further emphasises the predominant rôle played by crystal defects in the nucleation of microtwins. Attempts to remove these defects by prolonged annealing at high temperatures (700 to 1300°C) have proved unsuccessful. Hence, good quality device material can only be produced by either ensuring that specimens are cut to exclude regions of abnormally high twin density, or by growing crystals with a low twin density.

3.5. Crystals of Low Twin Density

Crystals with a uniform low twin density can be produced by preventing the formation of the defects which act as nucleation centres for the twins (see 3.2). Cellular structures are easily inhibited in $\text{Ba}_2\text{NaNb}_5\text{O}_{15}$ by lowering the growth rate of the crystal ($< 0.5\text{ cm h}^{-1}$). Growth striations can be controlled under low temperature gradient conditions [5]. Facet formation is less amenable to control, mainly because many low index planes can form facets in this material [9]. However, growth conditions producing an interface shape which is slightly convex towards

the melt are most favourable for avoiding facets in $\langle 001 \rangle_{\text{T}}$ axis crystals. Propagation of line defects from the seed is restricted by the growth of a long narrow neck to the crystal (approx 1 cm long \times 2 mm diameter).

A further improvement in the twin density has been achieved by using as-grown single crystals as the starting charge. Crystals grown from such charges exhibit a lower twin density (fig. 10) and are

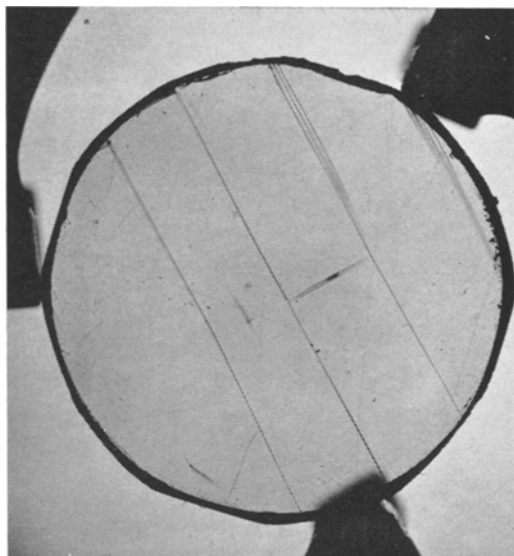


Figure 10 Twin density and distribution characteristic of regrown material.

deficient in both sodium and barium with respect to the original charge (table I). It is not at present known whether the low twin density arises from the greater purity of the re-grown material or from structural changes associated with the modified composition. There is some evidence that compositional changes within the barium sodium niobate ternary phase field can affect the twin density of the material. For instance, the twin density is reduced as the niobium content increases and for additions in excess of 10 wt % the crystals are twin free at room temperature. X-ray data show that these crystals are orthorhombic at room temperature

TABLE I

	Ba wt %	Na wt %	Nb wt %
Starting charge	27.4	2.3	46.4
Regrown crystal	28.0	1.6	46.6

so it appears possible for the tetragonal-orthorhombic transition to occur without twinning. These crystals are undoubtedly highly strained as they crack readily both during and subsequent to growth. Additions of barium (up to 5 wt %) and sodium (up to 10 wt %) do not produce any significant change in the twin density.

4. Conclusions

The main conclusions to be drawn from this work are as follows:

- (i) The density of the microtwinning in barium sodium niobate is greatly increased by the presence of defects produced at the liquid/solid interface during crystal growth: these include cellular structures, growth striae, defects propagating from the seed crystal and facets.
- (ii) The twin density can be reduced by suitable control of the major growth parameters in order to minimise growth defects. A further improvement appears possible by changing the composition within the ternary phase field of barium sodium niobate.
- (iii) The applied stress necessary to remove the microtwinning by compression during cooling through the tetragonal to orthorhombic transition is dependent upon the twin density and distribution.
- (iv) Rapid and pronounced changes in the dimensions of the tetragonal cell occur over the

temperature range 550 to 600° C. These changes afford a possible explanation for the increased tendency of the material to crack during heating or cooling through the Curie point.

Acknowledgement

This paper is published by permission of the Copyright Controller, HMSO. The authors wish to thank Professor G. V. Raynor, FRS for the provision of some of the laboratory facilities.

References

1. P. A. FRANKEN, E. A. HILL, C. W. PETERS, and G. WEINREICH, *Phys. Rev. Lett.* **7** (1961) 118.
2. J. A. GIORDMAINE and R. C. MILLER, *ibid* **14** (1965) 973.
3. L. G. VAN UITERT, J. J. RUBIN, and W. A. BONNER, *IEEE J. Quant. Elect.* **QE4** (1968) 622.
4. R. R. ZUPP, J. W. NIELSEN, and P. V. VITTORIO, *J. Cryst. Growth* **5** (1969) 269.
5. B. COCKAYNE, M. CHESSWAS, J. G. PLANT, and A. W. VERE, *J. Materials Sci.* **4** (1959) 565.
6. L. G. VAN UITERT, H. J. LEVINSTEIN, J. J. RUBIN, C. D. CAPIO, E. F. DEARBORN, and W. A. BONNER, *Mat. Res. Bull.* **3** (1968) 47.
7. B. A. SCOTT, E. A. GIESS, and D. F. O'KANE, *ibid* (1969) 107.
8. W. K. BURTON, N. CABRERA, and F. C. FRANK, *Phil. Trans.* **A243** (1951) 299.
9. B. COCKAYNE, J. G. PLANT, and A. W. VERE, to be published.